PL-TR-97-1110

X-RAY MEASUREMENTS WITH FILMS MASKED BY STAGGERED ABSORPTION LAYERS OF ALUMINUM

Thad J. Englert, Sue E. Englert, and James H. Degnan

January 1997

FINAL REPORT

APPROVED FOR PUBLIC RELEASE; DISTRIBUTION IS UNLIMITED.

20010419 094

AIR FORCE RESEARCH LABORATORY
Directed Energy Directorate
3550 Aberdeen Ave SE
AIR FORCE MATERIEL COMMAND
KIRTLAND AIR FORCE BASE, NM 87117-5776

PL-TR-97-1110

Using Government drawings, specifications, or other data included in this document for any purpose other than Government procurement does not in any way obligate the U.S. Government. The fact that the Government formulated or supplied the drawings, specifications, or other data, does not license the holder or any other person or corporation; or convey any rights or permission to manufacture, use, or sell any patented invention that may relate to them.

This report has been reviewed by the Public Affairs Office and is releasable to the National Technical Information Service (NTIS). At NTIS, it will be available to the general public, including foreign nationals.

If you change your address, wish to be removed from this mailing list, or your organization no longer employs the addressee, please notify AFRL/DEHP, 3550 Aberdeen Ave SE, Kirtland AFB, NM 87117-5776.

Do not return copies of this report unless contractual obligations or notice on a specific document requires its return.

This report has been approved for publication.

James H. Degnan

JAMES H. DEGNAN, Ph.D, DR-VI
Project Manager

FOR THE COMMANDER

COURTNEY D. HOLMBERG, Major, USAF
Chief, High Power Microwave Division

R. EARL GOOD, SES
Director, Directed Energy

REPORT DOCUMENTATION PAGE

Form Approved
OMB No. 074-0188

Public reporting burden for this collection of information is estimated to average 1 hour per response, including the time for reviewing instructions, searching existing data sources, gathering and maintaining the data needed, and completing and reviewing this collection of information. Send comments regarding this burden estimate or any other aspect of this collection of information, including suggestions for reducing this burden to Washington Headquarters Services, Directorate for Information Operations and Reports, 1215 Jefferson Davis Highway, Suite 1204, Arlington, VA 22202-4302, and to the Office of Management and Budget, Paperwork Reduction Project (0704-0188), Washington, DC 20503

1. AGENCY USE ONLY (Leave blank)	2. REPORT DATE	3. REPORT TYPE AND DATES COVERED
	January 1997	Final Report ; January 1996 – Januarry 1997

4. TITLE AND SUBTITLE
X-Ray Measurements with Films Masked by Staggered Absorption Layers of Aluminum

5. FUNDING NUMBERS
PE: 62601F
PR: 5797
TA: AQ
WU: 11

6. AUTHOR(S)
Thad J. Englert, Sue E. Englert, and James H. Degnan

7. PERFORMING ORGANIZATION NAME(S) AND ADDRESS(ES)
Air Force Research Laboratory / DEHP
Directed Energy Directorate
3550 Aberdeen Ave, SE
Kirtland Air Force Base, NM 87117-5776

8. PERFORMING ORGANIZATION REPORT NUMBER
PL-TR-97-1110

9. SPONSORING / MONITORING AGENCY NAME(S) AND ADDRESS(ES)

10. SPONSORING / MONITORING AGENCY REPORT NUMBER

11. SUPPLEMENTARY NOTES

12a. DISTRIBUTION / AVAILABILITY STATEMENT
Approved for Public Release; Distribution is Unlimited.

12b. DISTRIBUTION CODE

13. ABSTRACT ***(Maximum 200 Words)***
A technique for measuring x-ray emissions within the photon energy range 1 keV to 10 keV is described. A staggered set of aluminum absorbers, supported by kimfoil, is used to mask x-ray-sensitive film. Response functions of aluminum and kimfoil absorbers, along with the response function of the film, provide reasonable energy discrimination. Integrated incident energy along with modest spectral resolution may be obtained by convolution of the transmission of x-rays through the aluminum absorber stack and the exposed film density. Synthetic and experimental data are presented. For discrete photon energies, within the range noted, at least ±0.5 keV resolution is realized.

14. SUBJECT TERMS
x-ray emissions measurement 1 keV to 10 keV, kimfoil, x-ray sensitive film

15. NUMBER OF PAGES
36

16. PRICE CODE

17. SECURITY CLASSIFICATION OF REPORT	18. SECURITY CLASSIFICATION OF THIS PAGE	19. SECURITY CLASSIFICATION OF ABSTRACT	20. LIMITATION OF ABSTRACT
UNCLASSIFIED	UNCLASSIFIED	UNCLASSIFIED	UNLIMITED

NSN 7540-01-280-5500

Standard Form 298 (Rev. 2-89)
Prescribed by ANSI Std. Z39-18
298-102

Acknowledgements

The authors would like to express their gratitude to Dr. T.W. Hussey, Dr. B.L. Henke, Dr. G.F Kiuttu, and Dr. R.E. Peterkin for their comments, advice, and timely suggestions. Gratitude is also extended to Maj A.L. Chesley for his assistance in the preparation of this manuscript.

Table of Contents

Table of Figures

Tables

Abstract

A technique for measuring x-ray emissions within the photon energy range 1 keV to 10 keV is described. A staggered set of aluminum absorbers, supported by kimfoil, is used to mask x-ray-sensitive film. Response functions of aluminum and kimfoil absorbers, along with the response function of the film, provide reasonable energy discrimination. Integrated incident energy along with modest spectral resolution may be obtained by convolution of the transmission of x-rays through the aluminum absorber stack and the exposed film density. Synthetic and experimental data are presented. For discrete photon energies, within the range noted, at least ±0.5 keV resolution is realized.

I. Introduction

Photographic films sensitive to x-radiation have been used extensively in the diagnoses of plasmas[1-4]. Energy discrimination and/or spectral information is typically realized by filtering, bent crystals or grazing incidence gratings, or a combination thereof. The degree of film exposure subsequently provides a measure of the x-ray fluency, provided that the film sensitivity is known.

In this paper we describe a simple method for determining the primary constituents of low-energy x-radiation and the total associated energy, over a range of approximately 1 keV<hν<10 keV, generated from experiments at the SHIVA star capacitor bank facility of Phillips Laboratory. In these experiments a magnetized neon plasma is accelerated to approximately 20 cm/μs and stagnated against a target, resulting in generation of x-radiation. Kodak Direct Exposure Film (DEF), as described below, is exposed to the radiation for the duration of the stagnation. The purpose of the x-ray measurements described herein is to determine the amount of trans-kilovolt radiation generated during the plasma stagnation.

II. Description of Film Mask and Filtering

Figure 1 depicts the film holder along with the mask used in obtaining data. The mask consists of a staggered or "stair-step" stack of seven layers of 1.13 mg/cm^2 aluminum, plus a single strip of 2.05 mg/cm^2 aluminum which lies perpendicular to the staggered layers. This arrangement provides 14 different thicknesses of absorber through which the radiation passes before exposing the film. Support of the mask is provided by a thin (0.287 mg/cm^2) kimfoil whose stoichiometric formula is $C_{16}H_{14}O_3$. The effective thicknesses of the constituents of the kimfoil are 0.217

mg/cm^2, 0.0159 mg/cm^2, and 0.0542 mg/cm^2 for carbon, hydrogen and oxygen, respectively. Preceding the entire assembly is a 2.54×10^{-3} cm thick (4.69 mg/cm^2) beryllium window. From Figure 2 it may be seen that photons with energy less than about 1 keV are effectively filtered out by the beryllium before reaching the masked film arrangement. Those photons which are not filtered out by the beryllium suffer some attenuation by the kimfoil support. For a given x-ray photon energy E_v, with total intensity I_o incident onto the mask, the intensity, I_n, reaching the film becomes

$$I_n = \{I_o \exp[-\mu(E_v)\tau_n]\}T, \qquad (1)$$

where $\mu(E_v)$ is the absorption coefficient in cm^2/gm, τ_n is the combined absorber thickness for the nth ($0 \le n \le 14$) layer in gm/cm^2, and T is the transmission through the kimfoil support. If the incident radiation is not monoenergetic, some spectral discrimination may be realized, provided the absorption coefficients and kimfoil transmissions are sufficiently different for the photon constituents of the x-ray beam. The graph of Figure 3 shows the absorption coefficients in aluminum for photon energies of interest here. We can then say, by using Eq. 1, that for beams that contain photons of different energies the total intensity exposing the masked film through the nth absorber layer may be written

$$I_n = \sum_i \{I_{io} \exp[\mu_i(E_{iv})\tau_n]\}T_i, \qquad (2)$$

where the summation is taken over the discrete photon energies making up the x-ray beam.

Additional photon energy discrimination may be obtained since the film exposure is dependent on photon energy. Henke et al.[4] have determined the number of photons required to yield exposed DEF film densities (D) over the range $0.2 \le D \le 2.0$ for photon energies within 1 kev $\le E_v \le$ 10 keV. Figure 4 shows representative exposure curves for photon energies of 1 keV, 2.5 keV, 5 keV and 10 keV. Convolution of Eq. 2 with the film sensitivity functions should therefore provide an estimate of the photon energy and flux which leads to the measured film exposure.

III. Film Data and Analysis

No attempt was made at time resolution. The film was located ~1 m from the x-ray source and exposed for the duration of the plasma stagnation. Film developing followed the procedure as outlined by the manufacturer. Figure 5 shows

a digitized image of DEF film which has been exposed through the mask described earlier, along with an image showing grey-scale enhancement for ease of visualization. Film optical density is measured by scanning the original exposed film with a microdensitometer, determining the transmissivity (T_F) of the film, and calculating the film density (D) by $D = \log_{10}(1/T_F)$. Since the grain size in the DEF film is on the order of 1.6 μm (ref. 4), the densitometer was focused to a beam diameter of approximately 20 μm in order that noise due to graininess be smoothed. Density measurements performed on a Kodak standard density tablet, whose density range is $0.06 \leq D \leq 3.02$ in steps of ~0.15, show that a multiplicative correction factor of 0.65 must be applied to measurements made with the microdensitometer (See figure 6).

An iterative program is used to fit an arbitrary number of discrete incident photon energies to the experimental data. Polynomial functions are generated which separately describe the absorption coefficients in aluminum, transmission through the kimfoil support, and film response for each fitted photon energy. Some liberty has been taken with the data of reference 4 by extrapolating those results to 0.9 keV and 4.5 keV by using sixth-order polynomial equations. No results of fitting experimental data suggest the presence of photon energies above ~7.0 keV and fits containing photon energies greater than 7.0 keV are not presented here. It should be noted that photon energies corresponding to absorption edges in the mask, kimfoil support, and film constituents, have been avoided. The initial photon intensities, I_{i_0} (μm^{-2}) in Equation 2, are used as iterative parameters. Numbers of photons reaching the film, after passing through each aluminum absorber and kimfoil, are calculated and these photon numbers used to determine the resulting exposed film density, $D_{i,n}$ (Here n refers to the n^{th} absorber.). Calculated film densities are then added to determine the total film density according to

$$D_n = S_i D_{i,n} \qquad (3)$$

and comparison made between fitted film density, D_n(fit), and experimental film density, D_n(exp). This straight forward addition of film densities shown in Eq. (3) is likely not quite correct, due to the nonlinear nature of film, however no immediate alternative is obvious. Best fit is determined by minimizing $\Sigma_n[D_n(exp) - D_n(fit)]^2$. The results of fitting an array of photon energies, $0.9 \leq E_i \leq 7.0$ keV, with steps of ~0.2 keV are shown in Figure 7 and Table I. These results strongly suggest that 4.5-5.0 keV photons, and perhaps some amount of 1.5-2.0 keV photons,

are responsible for the film exposure. The best candidate(s) for the lower energy photons is multiply ionized iron (Fe^{+22} and Fe^{+23}) since the stagnation target was stainless steel. Several Fe^{+22} and Fe^{+23} lines lie within the range of 1.5 keV $\leq E_n \leq$ 2.0 keV. No immediate explanation for the presence ~5 keV photons has been found.

For completeness, Figure 8 and Table II show the best fit for the film region masked only by the seven-layered stack of 1.13 mg/cm^2 aluminum. The measured densities are somewhat more noisy than those found for the mask which included the 2.05 mg/cm^2 strip of aluminum however the fit supports the results of Figure 7 and Table I.

Assuming a uniform distribution over the entire solid angle, the total energy contained in the 4.5-5.0 keV radiation from the region of the stagnating plasma is only about 5 mJ. Similarly, for the 1.8 keV xrays, after accounting for transmission through the beryllium filter, a total of ~0.2 J of radiated energy from the stagnating plasma is seen.

IV. Simulations

Slight departures between the calculated and measured densities may conceivably be due to a mixture of photon energies with varying intensities. Indeed the entire set of observed film densities might be due to a continuum of x-rays with some appropriate intensity distribution. Unless the x-radiation is comprised of discrete photon energies separated by ~0.5 keV, or at least well separated absorption coefficients and film sensitivities giving clear breaks in the film density vs absorber thickness, it is not likely that better energy resolution than shown above is obtainable. By way of illustration, we consider several hypothetical cases, all of which assume the mask consists of the 2.05 mg/cm^2 strip overlaying the stack of 1.13 mg/cm^2 aluminum and supported by 0.28 mg/cm^2 kimfoil:

A. A beam of x-radiation is made up of discrete, reasonably separated, photon energies.

B. Black body continuum simulations.

C. An upper limit of detectability for 0.9 keV xrays is estimated and an upper limit of 0.9 keV xrays estimated for the experimental data.

A. Synthetic sets of DEF film exposures are generated for various combinations of up to four discrete photon energies. We then assume an incident flux of xrays, given by the sum of the individual fluxes incident onto the masked

film apparatus and calculate film densities after exposure through the mask and support. Since we do not anticipate better energy resolution than 0.5 keV, steps on the order of 0.2 keV have been used over the photon energy range $0.9 \leq E_i \leq 7.0$ keV for fitting the synthetically generated film exposure. Photon energies at absorption edges of the absorbers and film were again avoided. The resulting film density due to the simulated exposure from each x-ray energy used is assumed to be given by Eq. (3). As noted earlier, we recognize this simple addition as not being quite correct since density is not a linear function of exposure. The incident areal density (μm^{-2}) of each photon energy is a parameter which the program iterates until a best fit is obtained when compared to the synthetically generated film densities. A variety of combinations of photon energies were used in the generation of synthetic film exposures (densities) and in the iterative fitting of these data. Table III summarizes the results of four of these calculations and certain trends are evident. The fitting process usually introduces some amount of photon density at slightly lower energy. We believe that these contributions are due to small inaccuracies in the sixth-order polynomial functions used for calculating exposed film densities as functions of incident photon densities. It can also be seen that for incident photon energies whose aborption coefficients in aluminum, and transmission through the kimfoil, do not differ significantly (See fit for 1.5 keV, 3.2 keV, and 6.0 keV photons.), the simulations show greater uncertainty in the assignment of incident photon densities, however assignment of photon energies for best fit of simulated data are still well within the aforementioned resolution limits of ±0.5 keV. For xray energies that differ by ~0.3 keV but whose absorption coefficients are significantly different (See fit for 1.5 keV, 1.8 keV, and 6.0 keV photons.) it appear, from simulations, that the masked film technique should work very well.

B. Although the plasma in this experiment is not predicted to reach temperatures greater than several tens of eV [5], it seems worth while to consider the response of the masked film system to a continuum of radiation. Choosing 500 eV as a black body temperature, calculations have been made to determine the expected film density due to such radiation incident onto the masked film device. This temperature was chosen since the peak emission occurs around energies that are well suited for the masked film and that might also approximate the experimental data. The reader is reminded that a beryllium window precedes the aluminum mask and this will effectively filter out low energy radiation up to ~1 keV for the case of moderate intensities. The effects of the beryllium window are

included in these calculations. At 500 eV, the photon distribution from a black body falls off quickly as photon energies approach ~20 keV. The net effect is that the radiation incident onto the aluminum mask is peaked near a photon energy of 5 keV. Figure 9 shows the results of the black body calculation and compares it with the experimental results. It is unlikely that a stagnating magnetized plasma radiates exactly as a black body since the stagnation process is surely not an equilibrium state. However, it is clear that a continuum of incident radiation might yield the exposure which has been attributed to a beam made up of a few discrete photon energies.

To estimate the capability of the masked film device for response to coninuum sources, a simulated exposure has been calculated for radiation from a 500 eV blackbody. A least-squares fit of a blackbody distribution, with photon density and temperature as fitting parameters, has then been performed on the simulated exposure. Results of this simulation suggest that the device's response to a continuum is reasonably reliable, however the blackbody temperature determined by the fit, $430\ eV \leq T_{fit} \leq 450\ eV$ is slightly lower than the simulated temperature. Graphs of this simulation are found in Figure 10.

C. Although the DEF film has only been characterized for photon energies above 1 keV [4], it is useful to estimate the response of the masked film system to sub-kilovolt photons. Of particular interest are those xrays expected from helium-like neon (Ne^{+8}) since the primary constituent of the experimental plasma was ionized neon. The most intense radiation from Ne^{+8} is expected to be from the $1s^2$ - 1s2p configuration (0.913 keV). An extrapolation of the Henke data [4] in order to obtain DEF film response for 0.900 keV photons seems reasonable since there are no xray absorption edges within the range $0.9\ keV \leq E_n \leq 1.0\ keV$ for the film constituents. Such an extrapolation has been accomplished by a polynomial fit and is shown in Figure 10. Synthetic data are generated assuming fixed incident densities of 32.8 μm^{-2}, 0.30 μm^{-2}, and 0.30 μm^{-2} for 1.8 keV, 4.5 keV, and 5.0 keV photons, respectively, and densities of 10.0, 5.0, 1.0, and 0.5 μm^{-2} for 0.9 keV photons. In each case the assumption has been made that the film density due to each photon energy is simply additive. The results, shown in the bar graphs of Figure 11, suggest that fits for incident densities less than 1.0 μm^{-2} of 0.9 keV photons are not reliable (~50% error), even for errorless data. The apparent systematic error seen in the results are due to the choice of tolerance for the fit. Less error has been obtained, but not shown here, by requiring more stringent

tolerances of the fit routine. It is clear, however, that exposure due to more than one incident 0.9 keV photon/μm^{-2} would be readily discernable in conditions of low-noise film density. Figure 12 shows an overlay of the experimental data and synthetic data, assuming sufficient. 0.9 keV photons (20 μm^{-2}) to yield a film density corresponding to the maximum experimental error while keeping the 1.8 keV. 4.5 keV. and 5.0 keV incident fluxes fixed at~ worst~ fit values taken from Table 1 (33.0, 0.30, and 0.31 μm^{-2}, respectively). When the filtering effects of the beryllium window are accounted for, a maximum experimental total radiated energy due to 0.9 keV photons is found to be only ~1.7 J, assuming isotropic mission. The masked film device should therefore be able to determine rather low levels of radiation for photon energies around 0.9 keV in the presence of other higher, discrete photon energies.

The 0.9 KeV isotropic equivalent yield that is consistent with the filtered film array exposure data is ~ 1.7 joules. The viewing direction was normal to the axis of the cylindrical plate target, at approximately grazing incidence to the stagnation target surface, so the view may have been limited to target plasma before and after peak compression, rather than during peak compression or including the target surface itself. Data from other diagnostics with lines of sight at 120 to 180 degrees different azimuth indicated considerably higher isotropic equivalent yields at ~0.9 KeV. Two dimensional magneto-hydrodynamic simulations indicate that almost all of the radiation emission is from a region of the stagnated plasma that is very close to the target surface (< mm), and is emitted rapidly during peak compression. A slight tilt of the target surface could easily result in large anisotropy of observed emission during peak compression for this observation geometry.

Nevertheless, the filtered film array diagnostic technique is a simple, inexpensive, passive diagnostic that is a useful complement to other Vacuum Ultra Violet and X-ray diagnostics.

V. Conclusions and Discussion

The use of an aluminum mask arranged in steps of equal thickness has been used to provide variation in DEF film density due to x-ray exposure. The resulting film density is then compared to calculated film density based on aluminum absorber thickness and photon flux required to yield known exposed film optical densities. Results of this technique suggest photon energy resolution on the order of ±0.5 keV is possible for x-ray

beams comprised of few-keV photons. Exposed film density then allows an estimate of the total energy of the x-ray beam which exposed the film. Simulations indicate that less reliable photon numbers might be expected when absorption coefficients of the mask material have similar values.

Calculations also demonstrate that, under certain conditions, a continuum of radiation may yield nearly the same film exposure as a beam comprised of a few discrete photon energies for the absorber mask described here. It would be a simple matter, however, to discriminate between such scenarios by simultaneously using more than one absorber mask whose absorption characteristics differ sufficiently. The success of this technique clearly depends upon the widely differing responses of the absorber mask, kimfoil, and x-ray film to the radiation interacting with these components. It should be emphasized that the simulations presented here surely do not exhaust all possibilities. Of particular significance are those photon energies that coincide with absorption edges in absorbing materials and x-ray film. Future use of the masked film as an x-ray diagnostic should, in addition, use some material whose absorption edges are well removed from those of the materials used here. It would be a simple matter, for example, to include absorbers of aluminum on one half of the film and some other suitable material on the other half.

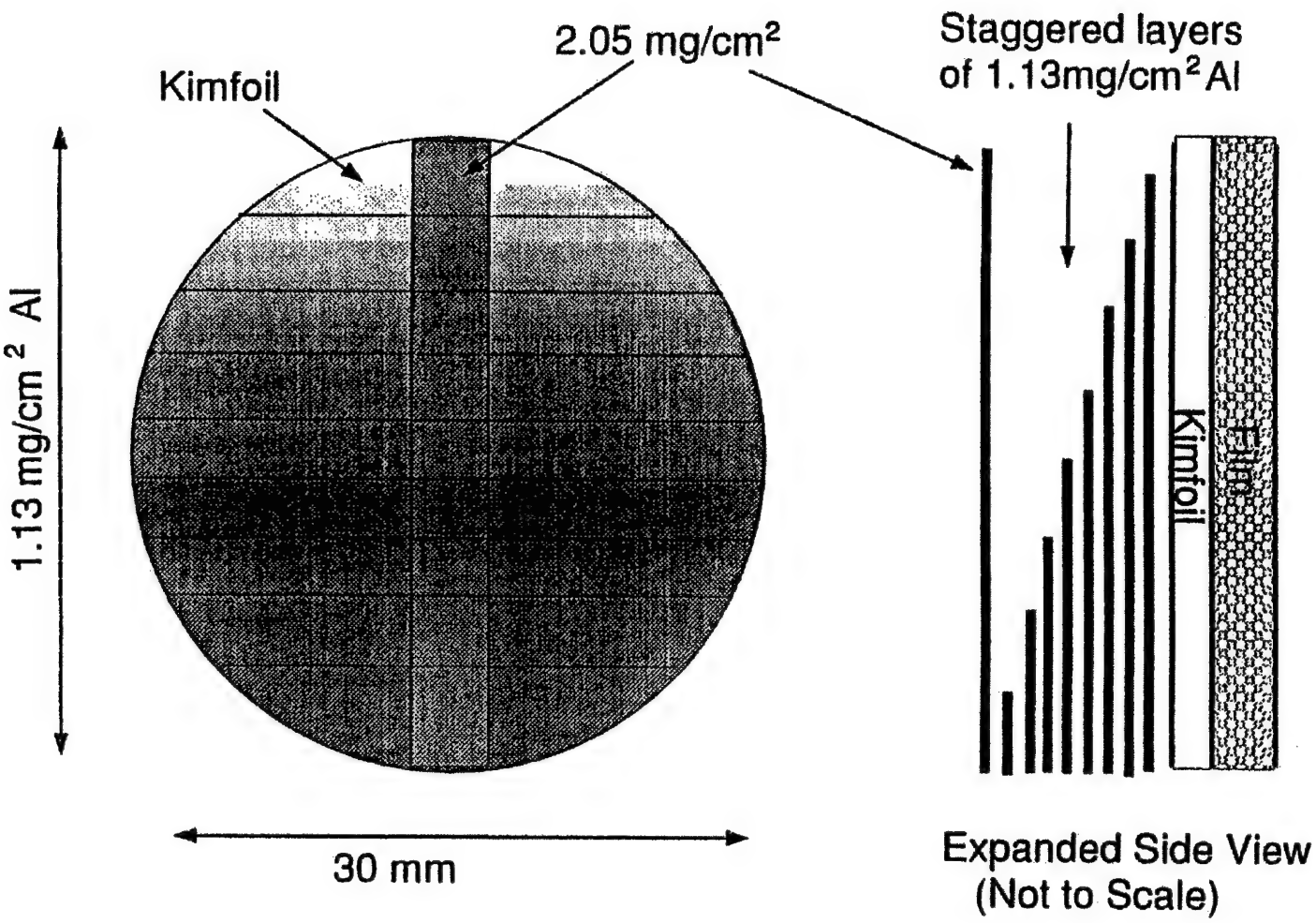

Figure 1. Schematic diagram depicting layered aluminum mask used to give variation if film exposure due to incident x-radiation.

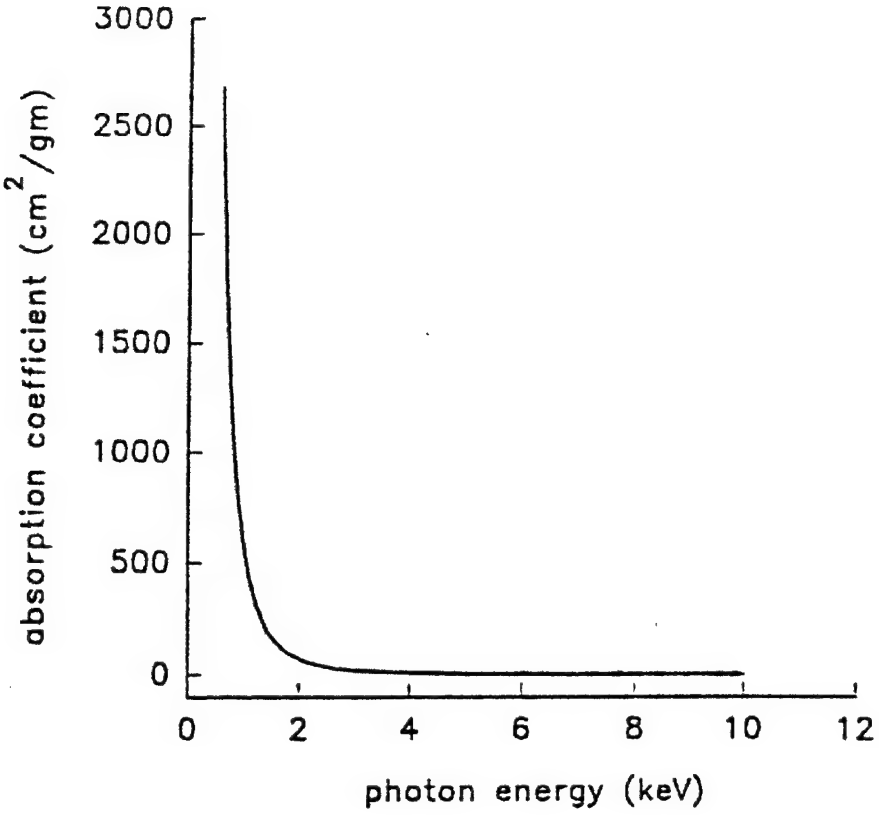

Figure 2. Absorption coefficient in beryllium for photon energies 0.6 keV≤E_v≤10 keV.

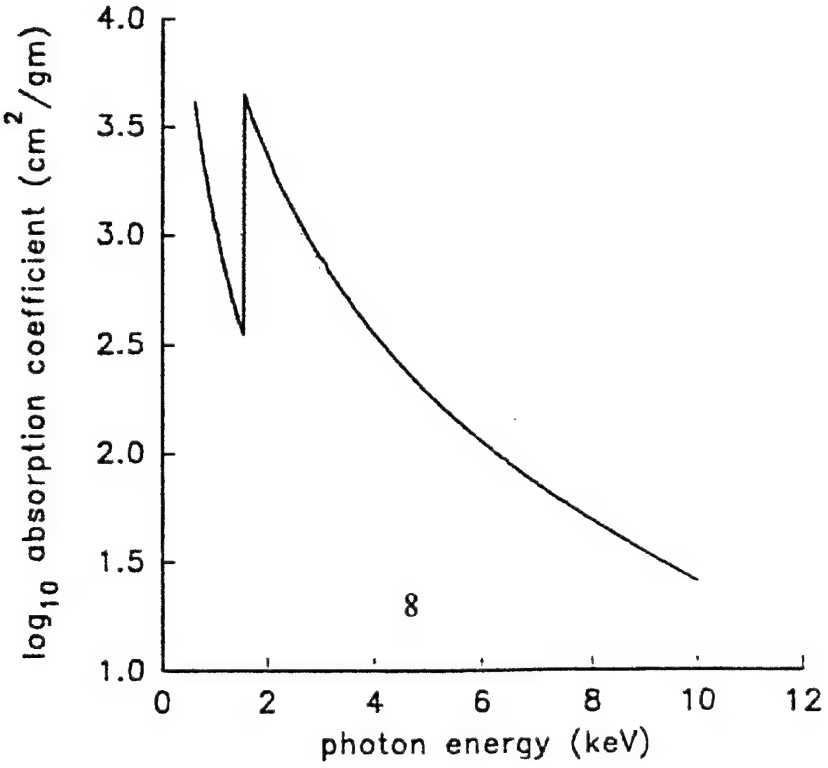

Figure 3. Absorption coefficient in aluminum for photon energies 0.6 keV≤E_v≤10 keV.

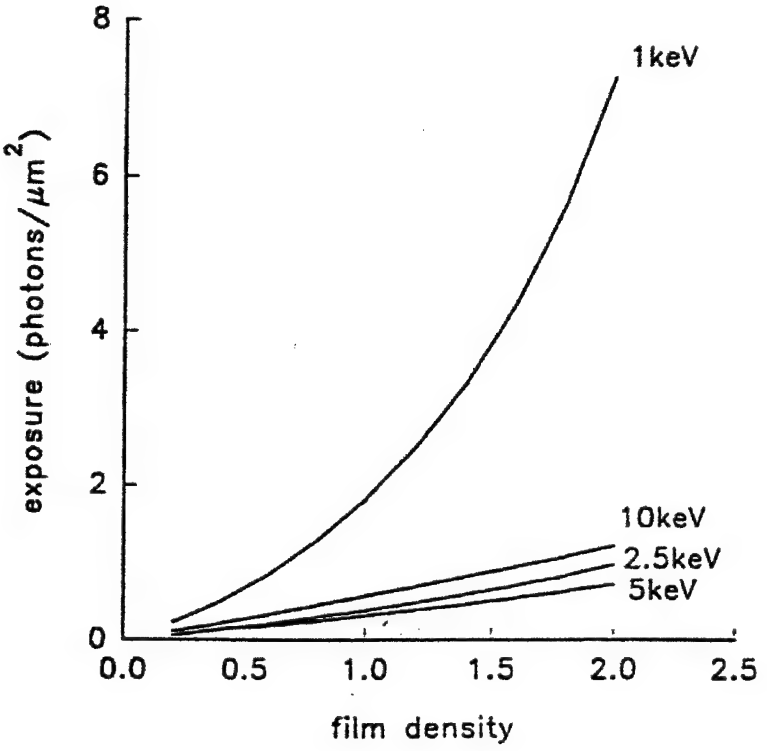

Figure 4. Representative curves showing incident photon density (μm^{-2}) required to expose DEF film (Henke[4] et al.).

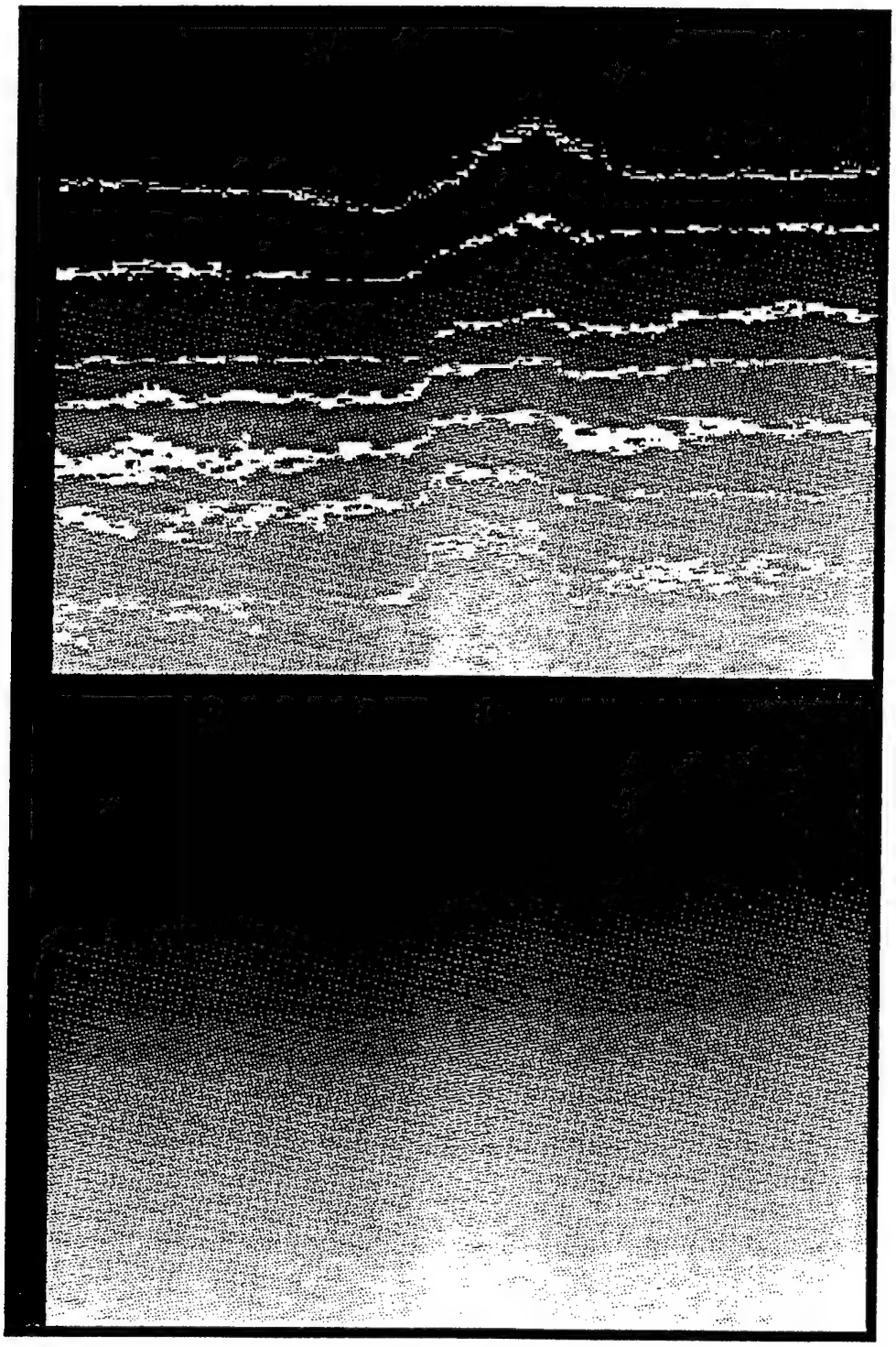

Figure 5. Top: Digitized sample of DEF film exposed by x-radiation, from stagnating magnetized neon plasma, after passing through the window and mask. Darkest area corresponds to greatest exposure.
Bottom: Computerized grey level enhanced view.
(For visualization purposes only.)

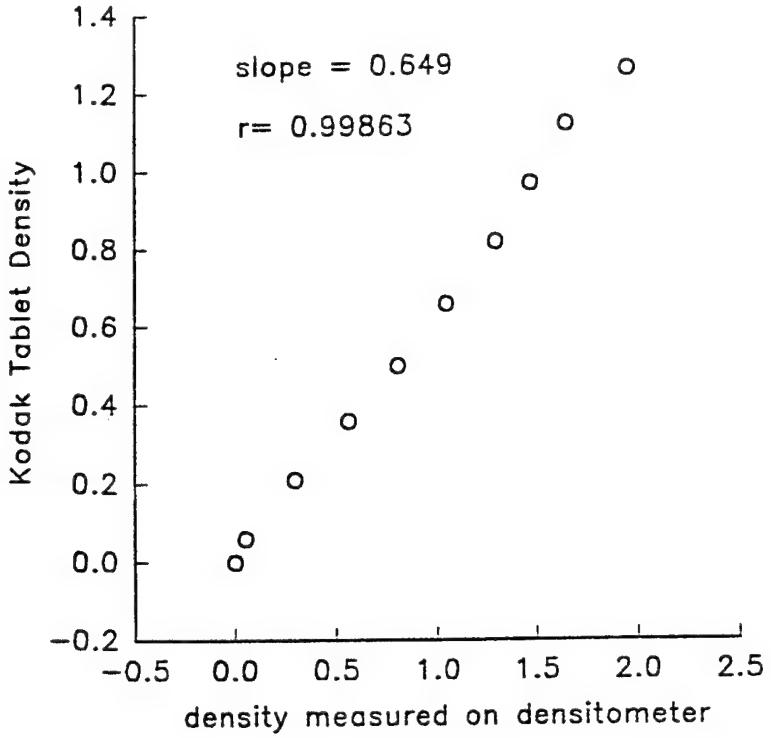

Figure 6. Graph of standard Kodak Tablet density vs that measured with the densitometer showing that densitometer measurements must be corrected by a factor of 0.65.

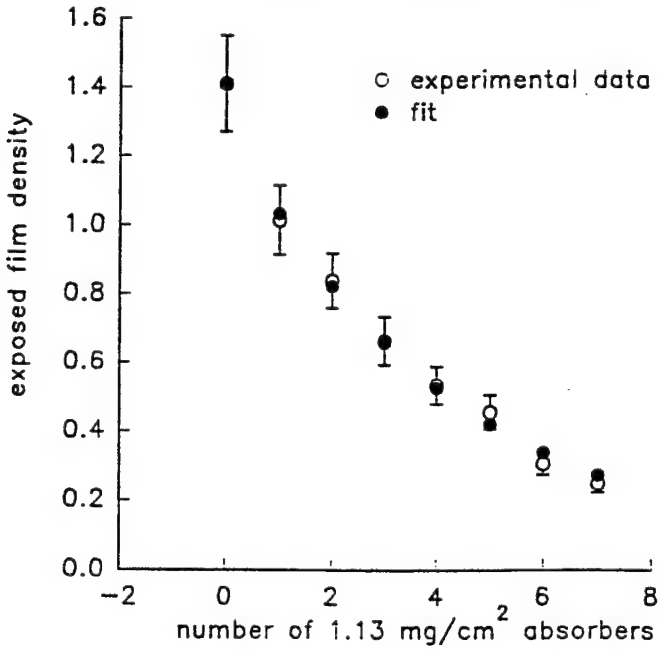

Figure 7. Experimental and fitted densities of DEF film exposed to x-radiation which has passed through a 2.05 mg/cm^2 aluminum strip, 7 staggered layers of 1.13 mg/cm^2 aluminum, and 0.287 mg/cm^2 kimfoil. Errors on experimental points are due to uncertainties in densitometer readings of the film.

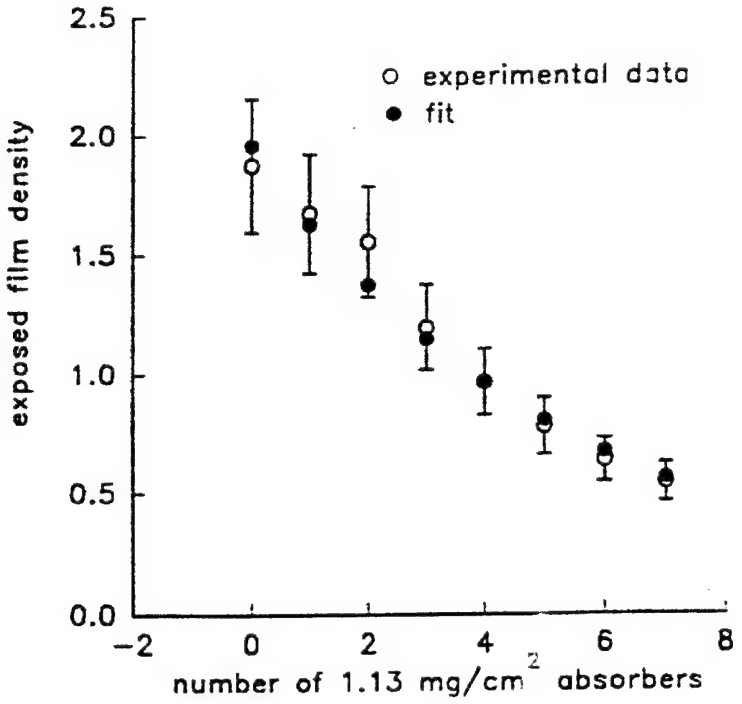

Figure 8. Experimental and fitted densities of DEF film exposed to x-radiation which has passed through 7 staggered layers of 1.13 mg/cm^2 aluminum and 0.287 mg/cm^2 kimfoil. Errors on experimental points are due to uncertainties in densitometer reading of the film.

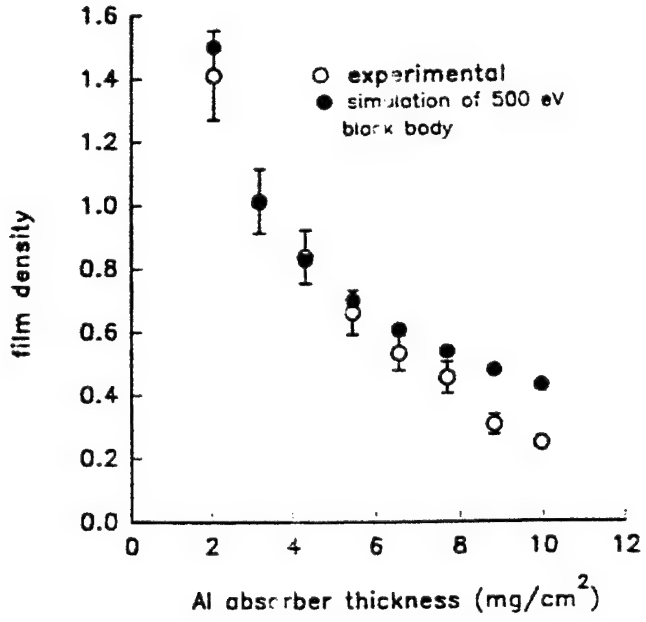

Figure 9. Graphical results comparing experimental film exposure due to the stagnating magnetized plasma and calculated exposure due to radiation from a 500-eV black body.

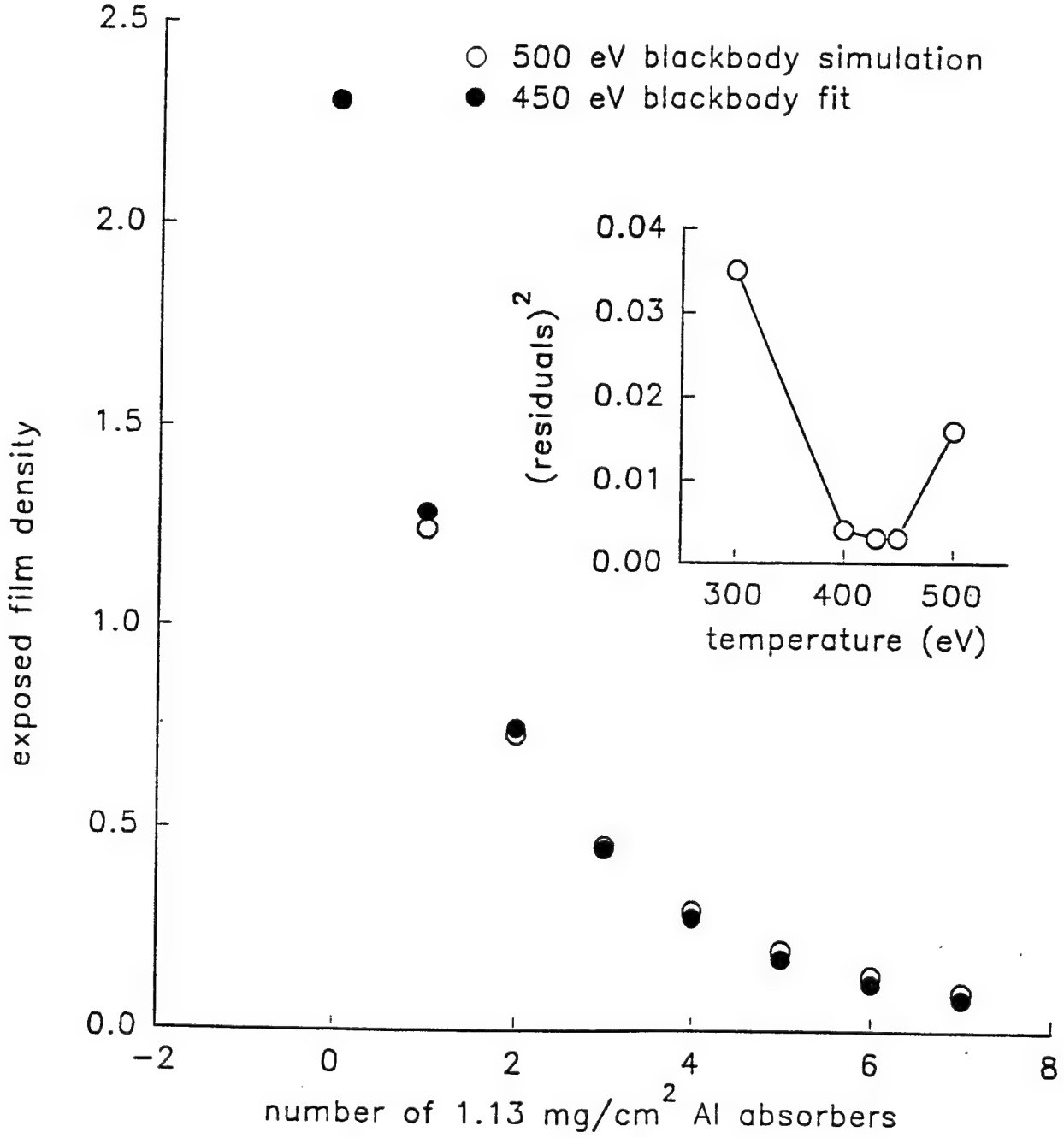

Figure 10. Results of simulated fit for exposure of masked fil to 500 eV black body radiation. Inset shows a plot of the sum of squared residuals between simulation and fit as a function of black body temperature.

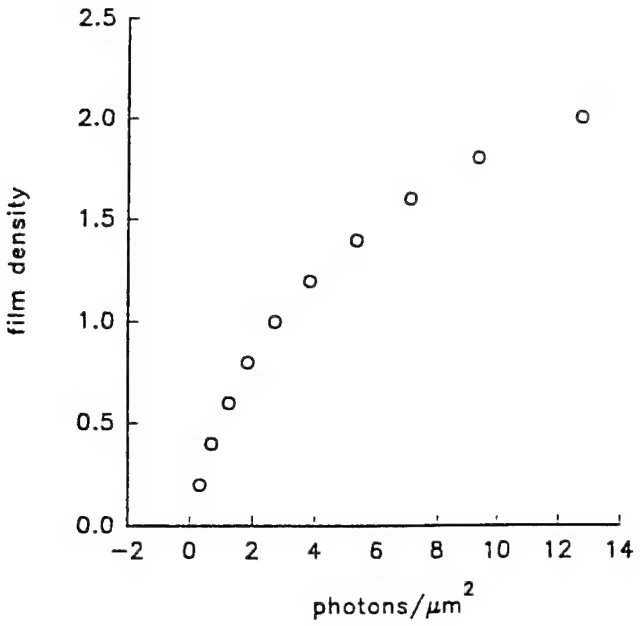

Figure 11. Extrapolation of Henke[4] data to 0.9 keV photons by using sixth-order polynomial fit.

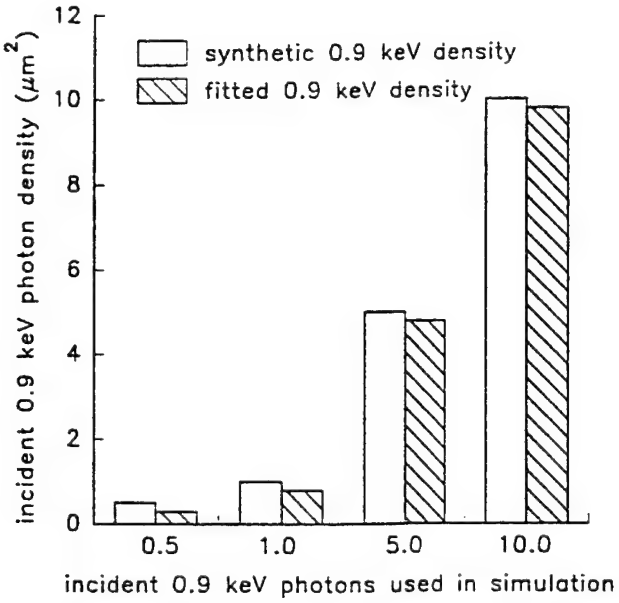

Figure 12. Estimation of lower limit of detectability of 0.9 keV x-rays from results of fitting a simulated x-ray exposure of DEF film through a 2.05 mg/cm^2 strip of aluminum, 7 staggered layers of 1.13 mg/cm^2 aluminum, and 0.287 mg/cm^2 kimfoil. In each case the 0.9 keV x-rays are mixed with 1.8 keV, 4.5 keV, and 5.0 keV x-rays with densities of 32.8 μm^{-2}, 0.30 μm^{-2}, and 0.30 μm^{-2}, respectively.

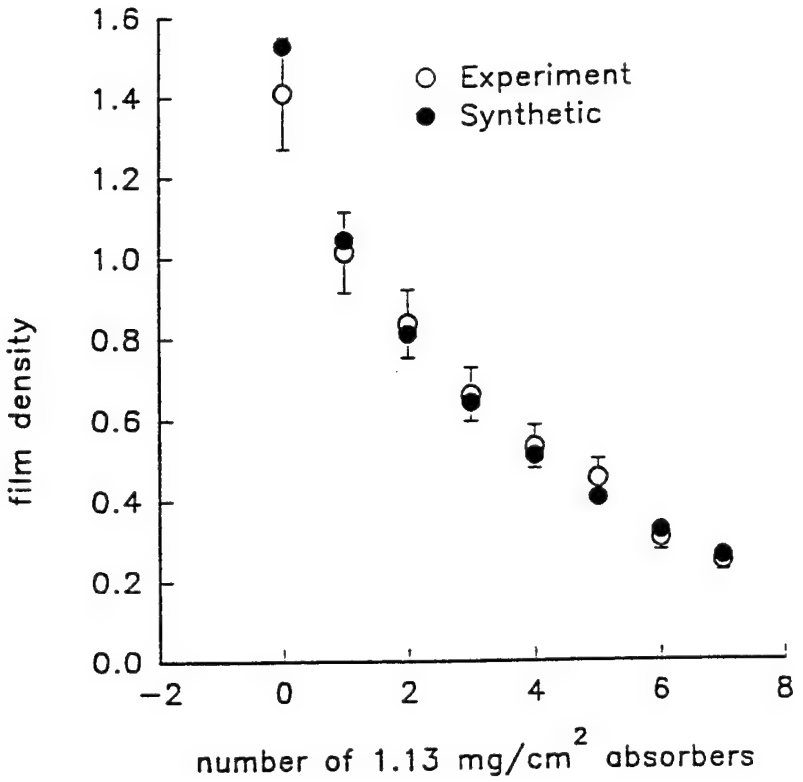

Figure 13. Comparison of experimental data and simulation estimating an upper limit for 0.9 keV radiation from the stagnating plasma. Calculated exposure is based on an incident density of 20.00 μm^{-2}, 33.00 μm^{-2}, 0.30 μm^{-2}, and 0.31 μm^{-2} for 0.9 kev, 1.8 keV, 4.5 keV, and 5.0 keV photons, respectively.

Table I. Fits of experimental data from 2.05 mg/cm^2 aluminum strip on 1.13 mg/cm^2 aluminum stack

photon energies fitted (keV)	fitted incident photon density (μm^{-2})	sum of square of residuals between fit and experiment
1.5	7.7(-08)†	
1.8	3.9(+01)	
2.0	1.9(-06)	
2.4	7.1(-07)	
2.8	4.3(-07)	
3.0	3.0(-07)	2.8(-03)
3.2	3.2(-07)	
4.0	2.5(-08)	
4.5	1.3(-01)	
5.0	4.8(-01)	
6.0	2.6(-09)	

Table 1. Continued

0.9	5.6(-07)	
1.2	2.4(-08)	
1.5	2.3(-09)	
1.8	3.4(+01)	
2.0	5.1(-08)	
2.2	4.0(-08)	
2.6	1.8(-08)	3.5(-03)
2.8	2.8(-08)	
3.2	5.4(-09)	
4.0	7.5(-10)	
4.5	2.5(-01)	
5.0	3.5(-01)	
6.0	9.3(-11)	

Table I. (continued)

0.9	3.5(-08)	
1.0	9.6(-09)	
1.4	3.6(-10)	
1.5	1.7(-10)	
1.8	3.3(+01)	
2.0	3.4(-09)	3.7(-03)
3.2	3.8(-10)	
4.0	5.6(-11)	
4.5	3.0(-01)	
5.0	3.1(-01)	
6.0	8.8(-12)	

†Numbers in parentheses denote exponent on 10.

Table II. Fit of experimental data from stack of 1.13 mg/cm^2 aluminum

photon energies fitted (keV)	fitted incident photon density (μm^{-2})	sum of square of residuals between fit and experiment
1.0	2.0(-07)†	
1.2	8.3(-08)	
1.4	3.4(-08)	
1.5	2.1(-08)	
1.8	3.2(00)	
2.0	1.1(-08)	6.1(-02)
2.6	2.5(-08)	
3.2	2.2(-08)	
4.0	8.2(-09)	
4.5	3.2(-09)	
5.0	5.2(-01)	
6.0	1.2(-01)	

†Numbers in parentheses denote exponents on 10.

Table III. Results of fits of simulated DEF film exposures through a 2.05 mg/cm^2 aluminum strip on a 7-layer stack of 1.13 mg/cm^2 aluminum.

photon energies used in fit (keV)	photon density used in simulation (μm^{-2})	photon density fitted (μm^{-2})	sum of squares of residuals between fit and simulation
0.9	0	6.9(+01)†	
1.0	10	5.3(-10)	
1.2	0	4.1(-10)	
1.4	0	1.5(-10)	
1.5	0	7.4(-11)	
1.8	0	1.5(+01)	8.9(-07)
2.0	20	9.0(+00)	
3.2	0	1.1(-10)	
4.0	0	2.4(-11)	
4.5	0	7.2(-02)	
5.0	0.6	5.3(-01)	
6.0	0	6.7(-12)	

Table III. (continued)

0.9	0	2.9(-15)	
1.0	0	3.4(-16)	
1.2	0	8.2(-18)	
1.4	0	5.3(-19)	
1.5	2.0	1.3(00)	
1.8	0	5.3(-15)	2.0(-07)
2.0	0	1.2(-15)	
3.2	0.5	2.7(-01)	
4.0	0	1.5(-01)	
4.5	0	2.9(-01)	
5.0	0.6	4.0(-01)	
6.0	0	4.6(-19)	

Table III. (continued)

1.0	0	1.6(-09)	
1.2	0	4.8(-10)	
1.4	0	1.2(-10)	
1.5	0	5.3(-11)	
1.8	0	5.9(+01)	2.0(-05)
2.0	20	6.5(00)	
2.6	0	1.1(-09)	
3.2	0	1.2(-10)	
4.0	0	1.7(-11)	
4.5	0	6.4(-02)	
5.0	0.8	7.2(-01)	
6.0	0	5.8(-12)	

Table III. (continued)

0.9	0	2.2(-15)	
1.0	0	3.3(-15)	
1.2	0	1.4(-16)	
1.4	0	9.8(-18)	
1.5	0.7	4.9(-01)	
1.8	0	1.0(-13)	2.2(-07)
2.0	0	1.8(-14)	
3.2	1.0	9.9(-01)	
4.0	0	1.5(-02)	
4.5	0	1.5(-11)	
5.0	0	1.3(-01)	
6.0	0.5	3.9(-01)	

†Numbers in parentheses denote exponents on 10.

References

1. C. M. Dozier, D. B. Brown, and L. S. Birks, "Sensitivity of x-ray film. II. Kodak No-Screen film in the 1-100 keV region". Journal of Applied Physics, Vol.47,No.8, 3732-3739, August 1976.

2. B. L. Henke, S. L. Kwok, J. Y. Uejio, H. T. Yamada, and G. C. Young, "Low-energy x-ray response of photographic films. I. Mathematical models". J. Opt. Soc. Am.B, Vol. 1, No.6, 818-827, December 1984.

3. B. L. Henke, F. G. Fujiwara, and M. A. Tester, "Low-energy x-ray response of photographic films. II. Experimental characterization". J. Opt. Soc. Am.B, Vol.1, No.5, 828-849, December 1984.

4. B. L. Henke, J. Y. Uejio, G. F. Stone, C. H. Dittmore, and F. G. Fujiwara, "High-energy x-ray response of photographic films: models and measurement". J. Opt. Soc. Am.B, Vol.3, No.11, 1540-1550, November 1986.

5. R.E. Peterkin, Phillips Laboratory, PL/WSP, Kirtland AFB, NM. private communication

DISTRIBUTION LIST

DTIC/OCP 8725 John J. Kingman Rd, Suite 0944 Ft Belvoir, VA 22060-6218	1 cy
AFSAA/SAMI 1570 Air Force Pentagon Washington, DC 20330-1570	1 cy
AFRL/VSIL Kirtland AFB, NM 87117-5776	2 cys
AFRL/VSIH Kirtland AFB, NM 87117-5776	1 cy
Official Record Copy AFRL/DEHP/James H Degnan, PH.D 3550 Aberdeen Ave SE Kirtland AFB, NM 87117-5776	2 cy